COMPARATIVE INVESTIGATION OF SHUNT ACTIVE POWER FILTERS IN 25kV AC ELECTRIFIED SYSTEMS

Han-Eol Park[1], Joong-Ho Song[2] , Wada Hosny[3]

1. *Dept. of Electric traction and Signalling Systems, Seoul National University of Technology, 172 Gongreung, Nowon, Seoul 139-743, Korea, email:haneo@snut.ac.kr*
2. *Dept. of Electrical Engineering, Seoul National University of Technology, 172 Gongreung, Nowon, Seoul 139-743, Korea, email: joongho@snut.ac.kr*
3. *CITE, University of East London, 4-6 university Way, Docklands, London, UK, email: wada@uel.ac.uk*

Abstract: AC electrified railway systems are embedded with power quality issues which include harmonic current pollution, feeder voltage perturbation and reactive power demand. This paper investigates comparatively two configurations of the shunt active power filter (SAPF) for improving the power quality in these systems. In addition, novel SAPF control algorithms based on the synchronous frame of reference are proposed. The effectiveness of the proposed SAPF control algorithms are illustrated via Matlab computer simulations and a comparative study on the two proposed configurations of SAPF has been carried out through a case study.

1. Introduction:

Currently power quality is a hot issue in electric power systems. This is because poor power quality not only causes energy loss within these systems but it could also result in the malfunction of the electric equipment integrated within and connected to these systems, (Moreno-Munoz et al, 2007). AC electrified railway systems typically show low power quality due to their inherent electrical characteristics. The dynamic and the non-linear load characteristic of the locomotives instigate the consumption of a considerable amount of reactive power and the production of harmonic currents. This in turn causes the power factor of the electric power systems supplying these locomotives to be low, (Battistelli et al, 2006) and (Sun et al, 2004). The power quality problems in the AC electrified railway systems delineated to above could have a detrimental impact on themselves as well as on all the other electric equipment connected to them, (Jinhao et al, 2008) . Therefore, a power quality compensator is required to improve the power quality in the AC electrified railway systems. Either passive or active power filters are used in order to improve the power quality in electric power systems. Passive power filters are simpler in construction and less expensive than active power filters. However, they are not suitable for the AC electrified railway systems because their compensation performance depends on these systems parameters and they incur resonance problems, (Salmeron et al, 2010). Research on active power filters have been carried out steadily due to their superior performance in comparison with passive power filter, (Corasaniti et al, 2009), (Luo et al, 2010) and (Tumbelaka et al, 2009). But there are few research investigations being carried out on active power filter for the AC electrified railway systems, in particular their location along

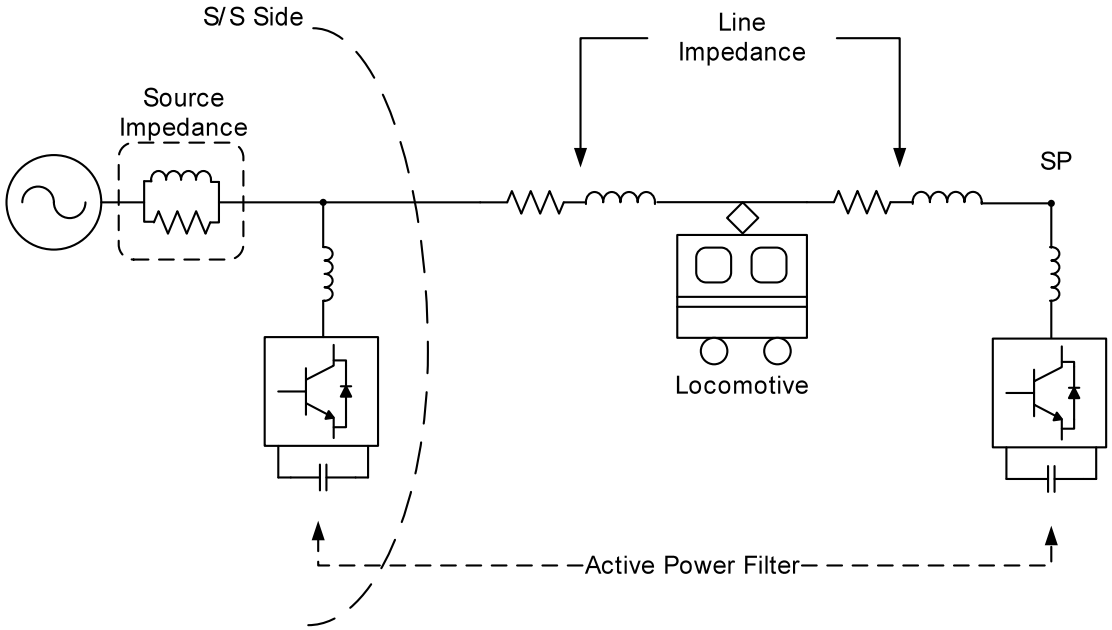

Fig.1 Possible locations of the SAPF for the electrified railway system

the railway distribution system for enhanced performance. As it can be seen in Fig.1, active power filters for an AC electrified railway system can be installed at two possible locations; either at the substation (S/S) side or at the sectioning post (SP) side. Thus, there are two possible configurations for implementing active power filters in this system depending on the locations of these filters along the railway electric distribution system. The purpose of this paper is to investigate the performance of these two different filter configurations as far as the improvement of the power quality of the railway electric power system is concerned. These two filter configurations require two different novel control algorithms. Therefore, they have different impact on the power quality improvement of these filters which is reported in this investigation. The novel control algorithms for these two filter configurations are based on the synchronous frame of reference and their effectiveness will be demonstrated via a case study.

2. Modeling of the AC electrified railway system:

An AC single phase electrified railway system is investigated in this paper, the distribution line circuit associated with this system is considered to constitute lumped circuits. The feeder line is represented by the circuit shown in Fig.2 consisting of three series π sections of resistance, R, in series with an inductance, L, and a parallel capacitance C. Each of these sections is 10 km long. The substation power supply is represented by an AC voltage source in series with internal impedance consisting of an inductance, L_s, in parallel with a resistance, R_s. As it is shown in Fig.1, the SAPF is composed of an inverter circuit, a harmonic filter to suppress the switching harmonics and a DC-link capacitor as an energy storage circuit component for the inverter loss. The locomotive is represented by a solid state AC to DC bridge converter.

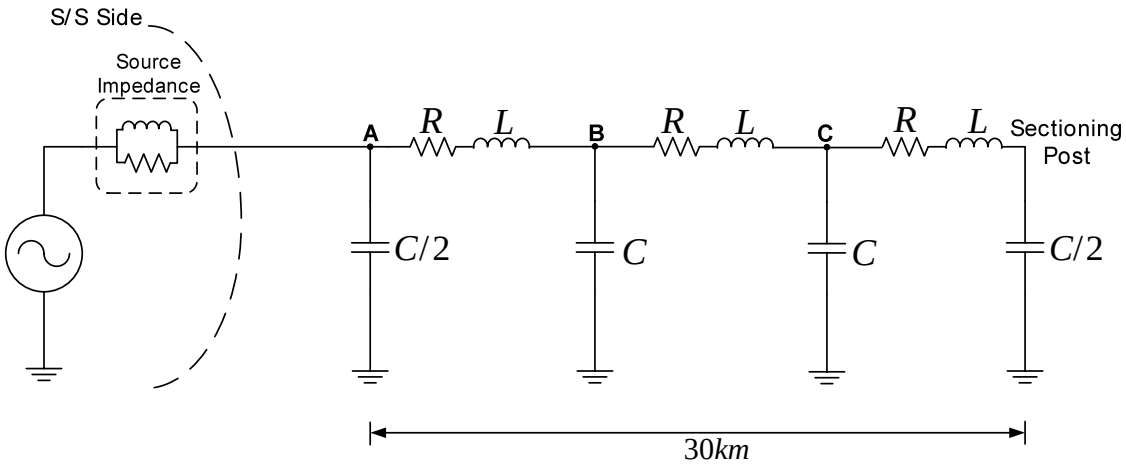

Fig.2 Modelling of the AC electrified railway system

3. Control of SAPF installed at the substation (S/S):

Fig.3 shows the AC electrified railway system with the SAPF provided at the substation. Thus, the electric system under investigation consists of the AC voltage source, the source impedance, the feeder line and the locomotive. The load current, i_L, is the current flowing into the locomotive. The load current, the SAPF current, i_{SAPF}, and the DC-link voltage, $V_{DC\text{-}link}$, are monitored for the active power filter controller input signals and the hysteresis control method is adopted for the current control of the filter.

3.1 Reactive power compensation algorithm:

The load current is expressed as follows:

$$i_L = I_L \cos(\omega t - \phi) \qquad (1)$$

where, I_L denotes the maximum value of the load current. This single-phase load current can be described in the stationary (α,β) or synchronous (d,q) frames of reference. Assuming that the supply voltage and load current vectors are positioned along the α-axis, and considering that the α and d axes are coincident, the supply voltage (voltage after the source impedance) and the load current components can be written as follows:

$$v_L = v_{L\alpha} = v_{Ld} \cos \omega t \qquad (2)$$

$$\begin{aligned} i_L &= i_{L\alpha} = i_{Ld} \cos \omega t - i_{Lq} \sin \omega t \\ &= I_L \cos\phi \cos \omega t + I_L \sin\phi \sin \omega t \end{aligned} \qquad (3)$$

It is obvious from Eq.(3) that the load current is decomposed into two components, one component (d-component) in phase with the supply voltage and another component (q- component) which is 90° phase-shifted with respect to the supply voltage. The active power current component, i_p, and the reactive power current component are defined as follows (Saitou et, 2003), (Tan et al, 2005) and (Hosny et al, 2008):

$$i_p = i_{Ld} \cos \omega t \qquad (4)$$

$$i_q = -i_{Lq} \sin \omega t \qquad (5)$$

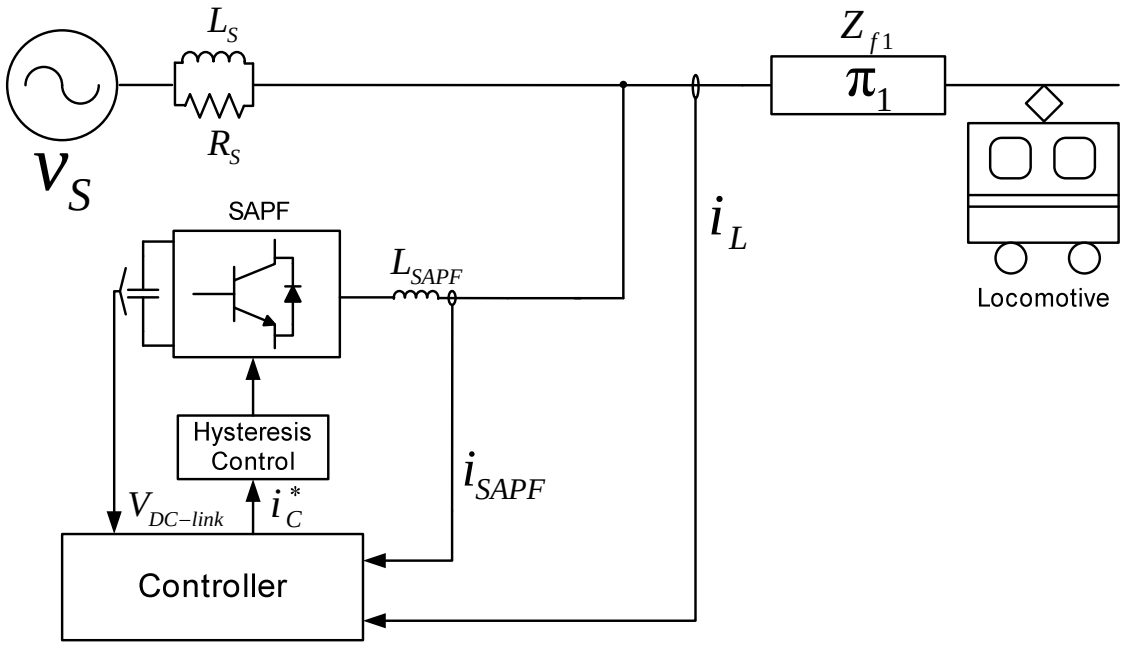

Fig.3 Structure of the AC electrified railway system when the SAPF is installed at the substation

Using equations Eqs.(4) and (5), the single-phase instantaneous active power, p(t), and reactive power, q(t), are represented as follows:

$$\begin{aligned} p_s(t) &= v_{L\alpha} \cdot i_p \\ &= v_{Ld} \cos\omega t \cdot i_{Ld} \cos\omega t \\ &= \frac{1}{2} v_{Ld} i_{Ld} \ 1+\cos(2\omega t) \\ &= V_{Lrms} I_{Lrms} \cos\phi \ 1+\cos(2\omega t) \end{aligned} \quad (6)$$

$$\begin{aligned} q(t) &= v_{L\alpha} \cdot i_q \\ &= -v_{Ld} \cos\omega t \cdot i_{Lq} \sin\omega t \\ &= -\frac{1}{2} v_{Ld} i_{Lq} \sin(2\omega t) \\ &= V_{Lrms} I_{Lrms} \sin\phi \sin(2\omega t) \end{aligned} \quad (7)$$

In Eqs.(6) and (7) V_{Lrms} and I_{Lrms} respectively represent the RMS values of the supply voltage and the load current. According to the above relations, the single-phase instantaneous active power depends solely on the d-axis current component and the single- phase instantaneous reactive power relies solely on the q-axis current component. Therefore, if the q-axis value of the current is forced to zero through controlling the q- axis current component, the reactive power can be compensated for. This control strategy for the SAPF is demonstrated in Fig. 4 which includes the block diagram for the reactive power compensation of the SAPF overall control scheme when it is installed at the substation. As it is clear from Fig.4, the source current, i_s, can be derived from adding the load current. I_L, to the filter current, i_{SAPF}. Thus, there is no need for an additional current sensor to monitor the source current.

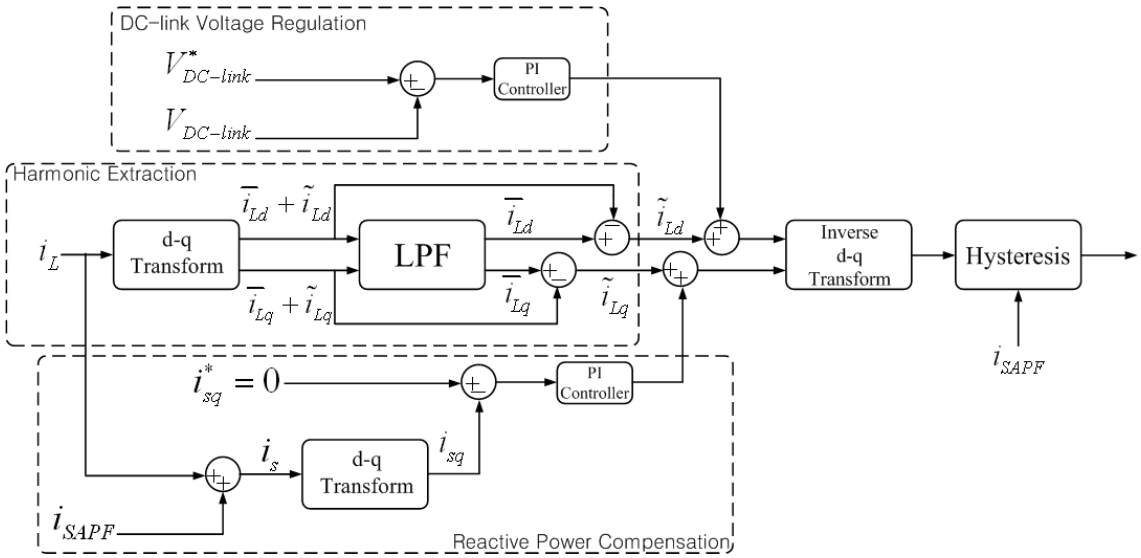

Fig.4 Overall control scheme of the SAPF when it is installed at the substation

3.2 Harmonic current extraction algorithm:

In this case, the d and the q components of the load current can be expressed as follows:

$$i_{Ld} = \bar{I}_{Ld} + \tilde{I}_{Ld} \quad (8)$$

$$i_{Lq} = \bar{I}_{Lq} + \tilde{I}_{Lq} \quad (9)$$

where, $\bar{I}_{Ld}$ and $\bar{I}_{Lq}$ respectively are the dc components of the d-q load current components. These components can be obtained using passive low pass filters. $\tilde{I}_{Ld}$ and $\tilde{I}_{Lq}$ respectively are the ripple or ac components of the d and q load currents. If the dc components of the load current d and q components are subtracted from the d-q load current components, this gives the d and q ripple current components of the currents to be compensated for. This control strategy is demonstrated in Fig.4 which includes the block diagram for the harmonic extraction in the SAPF overall control scheme when it is installed at the substation.

3.3 DC-link voltage regulation:

The dc link voltage regulator not only plays the role of voltage regulation, but it also compensates for the power losses within the SAPF. As it is clear from Fig.4, which includes the block diagram for the dc link voltage regulation, this voltage regulation process is included in the d-axis component of the load current control strategy within the SAPF.

4. Control of SAPF installed at the sectioning post:

Fig. 5 shows an alternative AC electrified railway system with the SAPF provided at the sectioning post (SP). In this case, the SP voltage, the SAPF current and the DC-link voltage are used as the filter controller input signals.

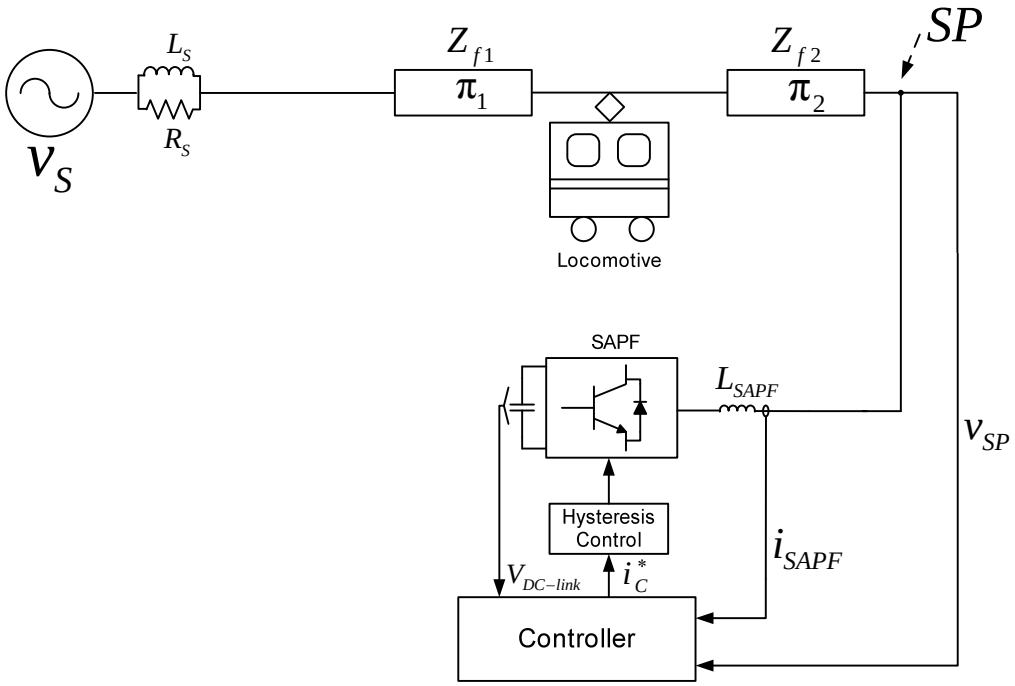

Fig.5 Structure of the AC electrified railway system when the SAPF is installed at the sectioning post

4.1 Reactive power compensation algorithm:

In this case, the voltage supplied to the locomotive is reduced due to the voltage drop across the feeding circuit impedance. This voltage drop is expressed as follows:

$$\Delta V = V_{S/S} - V_L \qquad (10)$$

Where, $V_{S/S}$ and V_L respectively denote the voltage at the substation and the locomotive, According to (Kawahara et al, 1997), the feeder line impedance can be expressed as:

$$\Delta V \approx I_L \times Z \times \cos(\theta - \gamma) = \frac{1}{V_{S/S}} \times (P_L R + Q_L X) \qquad (11)$$

Where:

I_L = the current flowing into the locomotive

θ = the angle between V_L and I_L

$Z = R + jX$

$\gamma = \tan^{-1}\frac{X}{R}$

$P_L = V_{S/S} I_L \cos\theta$

$Q_L = V_{S/S} I_L \sin\theta$

In Eq.(11), R and X depend on the feeder circuit characteristics but the active power, P_L, is determined by the power demand of the locomotive. R can be considered to be negligibly small in comparison with X. Hence, the voltage drop across the feeder line impedance dominantly depends on the reactive power, Q_L. Therefore, it can be deduced that the voltage drop can be indirectly compensated for by compensating for the reactive power (forcing it to approximately zero) with the aid of

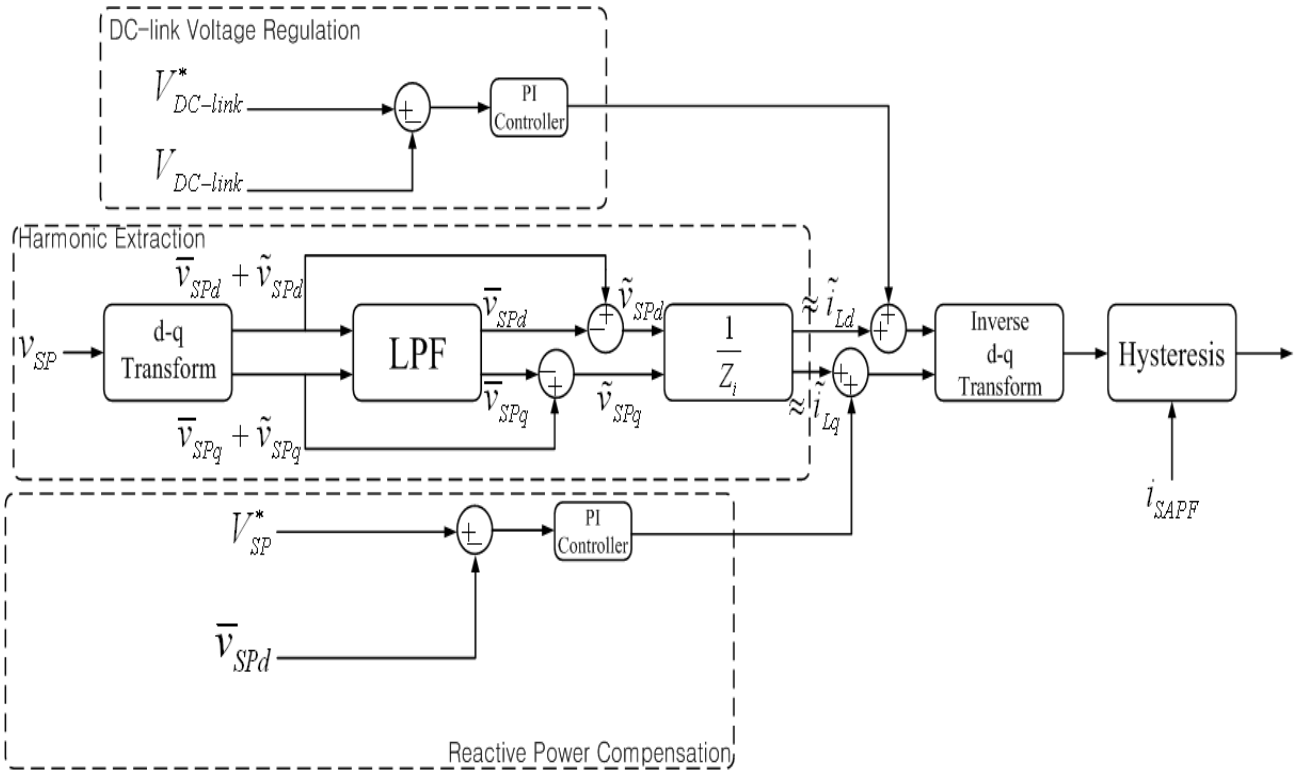

Fig.6 Overall control scheme of the SAPF installed the sectioning post (SP)

a reactive power compensator. The block diagram of this compensator is shown in Fig.(6) as part of the overall control scheme of the SAPF when it is installed at the sectioning post (SP). The d axis component of the supply voltage at the sectioning post (SP) consists of the dc component of this voltage together with some harmonic content. This dc component can be obtained using a passive low pass filter (LPF). In Fig.6, V^*_{SP} denotes the reference value of the SP voltage. As it was explained above, The error between $\bar{v}_{SPd}$ and V^*_{SP} is due mostly due to the reactive power flowing to the feeder line which could be compensated for using the PI-controller shown in this figure.

4.2 Harmonic voltage compensation algorithm:

The receiving voltage at the locomotive is influenced by the harmonic currents flowing into the locomotive. Therefore, the SP voltage is distorted and contains harmonic components. These harmonic voltage components are proportional to the harmonic load currents. The harmonic components of the SP voltage can be extracted as shown in Fig. 6. The harmonic load current, $\tilde{i}_L$, is obtained using the harmonic SP voltage and can be expressed as follows:

$$\tilde{i}_L \approx \frac{\tilde{v}_{SP}}{Z_i} \qquad (12)$$

where, $\tilde{v}_{SP}$ and Z_i respectively denote the harmonic SP voltage and the equivalent impedance of the feeding circuit. The optimal equivalent impedance can be determined by the trial and error method. The dc voltage regulator is added on the d-axis current control block diagram in the same manner as for the compensation system when the SAPF is installed at the substation.

5. Case study:

The electric power system under consideration is investigated together with the two possible configurations of the SAPF control algorithms delineated to above. This investigation is carried out using Matlab/ SimPowerSystems computer simulations. The selected system parameters for the simulations are extracted from (Tan et al, 2005) and are shown in Table 1.

Table 1 System parameters for case study

Source voltage	25kV, 60Hz
Filter inductor	5mH
DC-link capacitor	2500uF
Source impedance	1000Ω, 27.1mH
Pi-section line resistance	0.16Ω/km
Pi-section line inductance	0.14mH/km
Pi-section line capacitance	0.01uF/km

Table 2 shows the third harmonic distortion (THD) factor and the power factor of the source current with and without the installation of the SAPF. As it is demonstrated in this table, the power factor and the THD factor do not vary significantly according to the location of the locomotive away from the substation. It is also evident from this table that without the presence of the SAPF, the THD factor of the source current is as high as approximately 21% and the power factor is poor. When the SAPF is installed at the substation, Table 2 shows that the SAPF control algorithms proposed in this paper, enable the SAPF to effectively compensate for the harmonic current content in the load current. As it can be seen in this table, the THD factor of the compensated source current are well below 5% whereas as it was mentioned above the THD factor of the uncompensated source current is approximately 21%. Moreover, as it can be seen in Table 2, the power factor for the case when the SAPF is installed at the substation is close to unity. However, when the SAPF is installed at the sectioning post, Table 2 shows that the source current still has much reduced source current harmonic components than the source current without the installation of the SAPF, but it shows higher THD factor (about 11%) and lower power factor (about 0.97) than in the case when the SAPF is installed at the substation.

Table 2 THD and power factor

	10km	20km	30km
THD (without SAPF)	21.1	21.2	20.9
THD (with SAPF at S/S)	3.4	3.4	3.5
THD (with SAPF at SP)	11.4	10.9	11.2
Power Factor (without SAPF)	0.88	0.88	0.88
Power Factor (with SAPF at S/S)	0.99	0.99	0.99
Power Factor (with SAPF at SP)	0.99	0.97	0.97

Simulation results of the voltage drop across the feeder line versus the locomotive positions are now discussed. It is well known that the voltage drop is proportional to the distance from the substation to the location of the locomotive. When the SAPF

is not provided, and the locomotive is positioned near to the sectioning post (30 km away from the substation), the voltage drop is 2.7 kV. When the SAPF is installed at the substation the voltage drop at the locomotive is relatively reduced than in the case without the installation of the SAPF. The highest voltage drop occurs when the locomotive is farthest away from the SAPF. When the locomotive is 30 km away, the voltage drop is 1.8 kV, which is still considerable. On the contrary, when the SAPF is installed at the sectioning post, the voltage drop at the locomotive is quite low. It was also found out that the voltage drop at the locomotive is nearly zero when the locomotive approaches the sectioning post (30 km away from the substation)

6. Conclusions:

This paper presents a comparative study on the SAPF applications to the AC electrified railway systems and proposes novel control algorithms. The comparative study on two SAPF configurations is demonstrated via a case study. The performance of these two configurations alongside with their proposed control algorithms are evaluated for different locomotive locations. The simulation results demonstrated that the proposed SAPF control algorithms compensate for the power quality issues which include the harmonic current content pollution and the reactive power consumption. It is shown that when the SAPF is installed at the substation, it shows superior performance as far as the compensation for the current harmonic content and the reactive power (power factor close to unity). However, the feeder line voltage drop and the voltage sag at the locomotive cannot be fully compensated for. On the other hand, when the SAPF is installed at the sectioning post, the feeder line voltage drop and the voltage sag at the electromotive can be effectively compensated for. However, because the performance of the SAPF when it is installed at the sectioning post is inferior to that in the case when the SAPF is installed at the substation, as far as source harmonic current content and reactive energy compensation is concerned, the power rating capacity of the SAPF which is installed at the sectioning post is higher than that of the power rating capacity of the SAPF which is installed at the substation. It is concluded that the two SAPF configurations reported in this paper, offer different compensation characteristics for the electric power system under consideration. Therefore, it is absolutely vital that a proper appraisal of the available SAPF configurations alongside their control algorithms is carried out prior to installation in the electrified railway systems for power quality improvement.

7. References:

Moreno-Munoz, A., “Power Quality: Mitigation Technologies in a Distributed Environment”, Springer, 2007.

Battistelli,L, Lauria, D. and Proto, D., “Two-Phase controlled Compensator for Alternating Current Quality Improvement of Electrified Railway Systems”, IEEE Electr. Power Appl., Vol.153, pp.177-183, 2006.

Sun, Z., Jiang, X., Zhu, D.and Zhang, G., “A Novel Power Quality Compensator Topology for Electrified Railway”, IEEE Trans. Power Electronic, Vol.19, pp.1036-1042, 2004.

Jinhao, W., Lei, X., Yuzhuo, L., Mengzan, L., Leilei, P., Shuying, L., Shuzhong, W., and Yingying, L. “The Interaction Research

Between Public Grid and Traction Power Supply System," *IEEE Int. Conf. Electricity Distribution*, 2008, pp.1-8.

Salmeron, P., and Litran, S. "Improvement of the electric power quality using series active filter and shunt passive filter," IEEE Trans. Industrial Electron., vol. 25, pp.1058-1067, 2010.

Corasaniti, V., Barbieri, M., Arnera, P., and Valla M. " Hybrid Active Filter for Reactive and Harmonics Compensation in a Distributed Network", IEEE Trans. Industrial Electronics, Vol.56, pp.670-677, 2009.

Luo, A., Shuai, Z., Zhu, W., Shen, Z., and Tu, C. "Design and Application of a Hybrid Active Power Filter with Injection Circuit," IET Electronic Power Appl., Vol. 3, pp. 54-64, 2010.

Tumbelaka, H., Borle, L., Nayar, C., and Lee, S. "A Grid Current-Controlling Shunt Active Power Filter", KIE J. Power Electronic, Vol.9, pp.365-376, 2009.

Saitou, M., Matsui, N., and Shimizu, T. "A Control Strategy of Single-Phase Active Filter using a Novel d-q Transformation," IEEE Int. Conf. Ind. App*l.*, pp. 1222-1227, 2003

Tan, P., Loh, P., and Holmes, D. "Optimal Impedance Termination of 25kV Electrified Railway Systems for Improved Power Quality," IEEE Trans. Power Deliv., Vol.20, pp.1703-1710, 2005.

Hosny, W. and Dobrucky, B., "Novel Strategy for Compensating current determination in Single Phase Active power filters", Wseas International Conference on Energy & Environment (EE'08), University of Cambridge, Cambridge, UK, pp.319-323, 2008.

Kawahara, K., Hase, S., Mochinaga, Y., and Hisamizu, Y. "Compensation of Voltage Drop using Static Var Compensator at Sectioning Post in AC Electric Railway", IEEE Int.Conf., Power Conversion, pp.995-960, 1997.